Miscibility in Cyclic Poly(butylene terephthalate) and Styrene Maleimide Blends Prepared by Solid-Dispersion and *In Situ* Polymerization of Cyclic Butylene Terephthalate Oligomers within Styrene Maleimide

Sani A. Samsudin,[1,2] Stephen N. Kukureka,[2] Mike J. Jenkins[2]

[1]*Faculty of Chemical Engineering, Universiti Teknologi Malaysia, 81310 UTM Skudai, Malaysia*
[2]*College of Engineering and Physical Science, School of Metallurgy and Materials, The University of Birmingham, Edgbaston, Birmingham B15 2TT, United Kingdom*

Received 2 August 2011; accepted 30 January 2012
DOI 10.1002/app.36918
Published online in Wiley Online Library (wileyonlinelibrary.com).

ABSTRACT: Blends of cyclic butylene terephthalate oligomers (CBT) and styrene maleimide (SMI) were prepared by a solid dispersion technique in various compositions ranging from 90 to 10 wt % of CBT. *In situ* polymerization of the oligomers in the blend at 190°C produced a blend of cyclic poly(butylene terephthalate) (c-PBT) and SMI. The blends were characterized by a variety of techniques including differential scanning calorimetry (DSC) and scanning electron microscopy (SEM). It was found that the presence of 30 wt % and above of SMI impeded the crystallization of c-PBT to such an extent that crystallization could not be detected under the conditions of the DSC experiment. The blend system exhibited a single composition-dependent glass transition temperature (T_g), which indicated the presence of miscibility. © 2012 Wiley Periodicals, Inc. J Appl Polym Sci 000: 000–000, 2012

Key words: cyclic butylene terephthalate oligomers; styrene maleimide; blends; miscibility; differential scanning calorimetry

INTRODUCTION

Cyclic butylene terephthalate (CBT) is low-molecular weight cyclic oligomer that can be produced by the depolymerization of linear, high-molecular weight poly(butylene terephthalate).[1–4]. CBT oligomers have many useful properties including a particularly low melt viscosity (≈17 mPa s, water-like), which makes the polymer of particular interest in the production of composite materials.[5–9] The presence of low viscosity cyclic oligomers (CBT) overcomes the problems of high viscosity thermoplastic matrices which always hamper fiber impregnation. The low viscosity also allows the use of production techniques normally associated with thermoset composites such as resin transfer molding (RTM). CBT can also be used for the production of textile-reinforced thermoplastics.[10,11] The chemical structure of CBT oligomers is shown in Figure 1.

CBT oligomers can be polymerized via a ring-expansion process in the presence of a suitable catalyst such as stannoxane. In the case of a stannoxane catalyst, polymerization can be achieved by heating the oligomers to a temperature of 190°C and holding for a time of 3–5 min.[9] The polymerization is said to be athermal and cannot be detected by differential scanning calorimetry (DSC); however, DSC is able to detect the crystallization process of the cyclic polymer which is believed to occur simultaneously with the polymerization process.[12]

Although the aim of commercial production of cyclic oligomers is largely for liquid-molding applications, they are also currently receiving some attention in three main areas; polymer blends,[13–15] composites,[16–20] and nanocomposites.[21,22] Cyclic polymers produced from cyclic oligomers offer unique possibilities for processing by combining *in situ* polymerization of the cyclic oligomers with the blending process. These blends can be miscible[14] or immiscible[13,15] and may produce some interesting features not seen with linear polymers. For example, Nachlis et al.[13] found that the *in situ* polymerization of bisphenol-A-carbonate cyclic oligomers (BPACY)/styrene-acrylonitrile copolymer (SAN) blends could produce nanocomposite structures through liquid–liquid phase separation. These morphologies were unattainable via conventional melt blending.

Styrene maleimide (SMI) is a low-molecular weight (M_w = 5000–10,000) synthetic copolymer that is composed of styrene and dimethylaminopropylamine (DMAPA) maleiamide (Fig. 2). This

Correspondence to: S. A. Samsudin (saniamril@cheme.utm.my).

Contract grant sponsors: Ministry of Higher Education Malaysia (MOHE), Universiti Teknologi Malaysia (UTM).

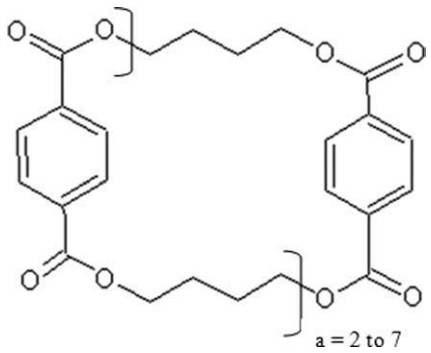

Figure 1 Structure of CBT oligomers.

copolymer is formed by a radical polymerization using organic peroxide as the initiator. SMI has a low melt viscosity, a high level of tertiary amine functionality, high thermal stability (where the decomposition temperature is greater than 300°C), and a low volatile organic compounds (VOC) content. SMI can also function as a polyimide or polyamine additive, serving as a crosslinking agent, curing catalyst, or surface modifying agent. The typical uses of this copolymer include paper manufacture, alkali resistant coatings, adhesives, and polymer modification.

To date, the cyclic poly(butylene terephthalate) and styrene maleimide (c-PBT/SMI) blend system has not received any attention in the literature, and therefore, this blend system will form the basis of this study. Given the fact that both blend components exhibit particularly low melt viscosities, the blends will be prepared using a solid-dispersion technique. This preparation method will allow the polymerization of CBT to take place from within the blend (post preparation) rather than during the blending process which would otherwise occur during a conventional melt-blending process. The miscibility of the resulting c-PBT/SMI blend will be explored through the compositional variation of the SMI glass transition temperature and the variation of the equilibrium melting point of c-PBT. The extent of any miscibility will be further characterized using the approach developed by Nishi and Wang[23] and Nishi et al.[24]

EXPERIMENTAL

Materials

Cyclic oligomers of butylene terephthalate (CBT), (XB2-CA4) of molecular weight $M_w = (220)_n$ (with $n = 2$–7) in powder form were provided by the Cyclics Corporation (2135, Technology Drive, Schenectady, New York 12308, US) (www.cyclics.com). The XB2-CA4 contained the stannoxane catalyst and was termed a one-component CBT, where the resin and catalyst were premixed. The general procedures for combining CBT and catalyst are described in a US patent assigned to Cyclics Corporation.[25] These materials were dried in a vacuum oven for 24 h at 90°C prior to processing. The styrene maleimide (SMI 1000I) with M_w ranging from 5000 to 10,000 also in a powder form was supplied by the Sartomer Company (502 Thomas Jones Way Exton, PA 19341, US) (www.sartomer.com).

Sample preparation

A powder mix of CBT and SMI was produced in various compositions ranging from 90 to 10 wt % of CBT. The powder blends were mixed in an agate mortar and pestle until a homogeneous blend was observed. This observation was facilitated due to the color difference between the component powders: SMI was yellow and CBT was white. The rationale for adoption of the solid dispersion technique is twofold. Firstly, the blend components exhibit very low viscosity so will disperse easily in the melt. Furthermore, had a melt extrusion process been adopted it would allow polymerization to occur during the mixing process which may induce or allow premature phase separation. Conversely, solid dispersion prior to polymerization allows the phases to be well dispersed prior to polymerization.

Differential scanning calorimetry

Thermal behavior of the blends

The thermal behavior of the CBT/SMI blends was measured using a Perkin–Elmer differential scanning calorimeter (DSC-7) interfaced to a PC running Pyris software. Experiments were run at a heating rate of 10 °C min^{-1} and a sample mass of 20 mg was adopted for all experiments. A nitrogen purge gas (flow rate of 20 cm^3 min^{-1}) was used to minimize any thermal degradation.

Isothermal crystallization during polymerization of CBT

With the aim of understanding the simultaneous crystallization and polymerization processes which

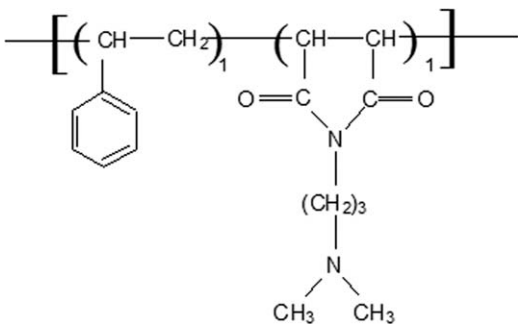

Figure 2 Structure of SMI resin.

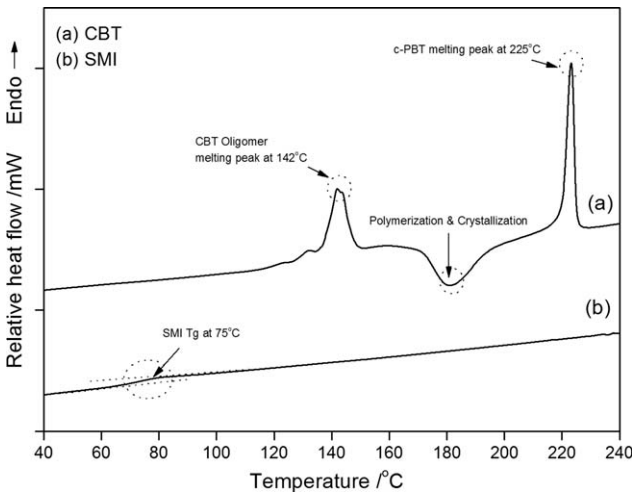

Figure 3 Typical DSC dynamic heating trace of CBT and SMI.

occur after the melting of CBT, a sample of CBT was rapidly heated (100 °C min^{-1}) to an optimum polymerization temperature of CBT, i.e., 190°C. The sample was then held at the target temperature until the crystallization curve returned to the baseline.

Glass transition temperature (T_g) measurement

Blend samples were heated rapidly to the polymerization temperature (190°C) and held at that temperature for 10 min. Following this isothermal hold, the sample was then heated to above the c-PBT melting point and removed from the DSC to enable a rapid quench into liquid nitrogen. This ensured that both blend components were amorphous. The glass transition behavior of the blend was examined by returning the sample to the DSC and heating from −10°C to 240°C at 10 °C min^{-1}. Given that no endothermic peaks were detected for the glass transition processes, the glass transition temperatures were measured from the midpoint of the inflection of the variation of relative heat flow with temperature. Measurement of ΔC_p was enabled by using the widely accepted procedure involving a series of baseline subtractions.[26]

Scanning electron microscopy

Samples suitable for scanning electron microscopy (SEM) were created by polymerizing a sample of CBT/SMI at 190°C within a rectangular mold. The isothermal hold times were as follows, 5, 10, 30, and 60 min. The purpose of varying the hold time at this temperature was to enable the investigation of the effect of *in situ* polymerization on the blend morphology. The resulting samples were then immersed in liquid nitrogen for a period of 2 min prior to fracture. The fracture surfaces were coated in gold using a Polaron E5000 sputter coater. Scanning electron micrographs were recorded using a JEOL JSM-6060LV at accelerating voltages of 20 kV.

RESULTS AND DISCUSSION

Thermal behavior of the blends

Typical DSC traces for CBT oligomers and SMI are shown in Figure 3. It can be seen that two melting peaks are apparent for the 100 wt % CBT oligomers. The first melting peak was observed at 142°C and it is well known that this peak corresponds to the melting of CBToligomers.[27,28] At this temperature, the CBT shows a phase change from solid to low viscosity liquid. The breadth of the oligomer melting region has been explained in terms of a wide distribution of oligomers within the sample.[28] Furthermore, a previous study found that CBT oligomers obtained via depolymerization comprised of different proportions of oligomers indicated by slightly different melting temperatures.[29]

After the melting process was complete, the CBT oligomers are understood to have undergone concurrent crystallization and polymerization in the temperature range 170–215°C, where crystallization appears as a dip in the heating trace at 180°C. Brunelle and Shannon,[30] who extensively investigated the polymerization of CBT oligomers using tin and titanium catalysts found that the 0.25 wt % of stannoxane catalyst allowed the CBT polymerization to be completed within 2–3 min at 190°C. The *in situ* polymerization produces the c-PBT which subsequently melts at 225°C. The thermal response of SMI is also shown in Figure 3 (trace b). The only thermal transition is the glass to liquid transition, which was observed at 75°C. SMI can therefore be confirmed as an amorphous polymer.

Figure 4 shows the initial thermal response of the blends of CBT/SMI after the solid dispersion phase.

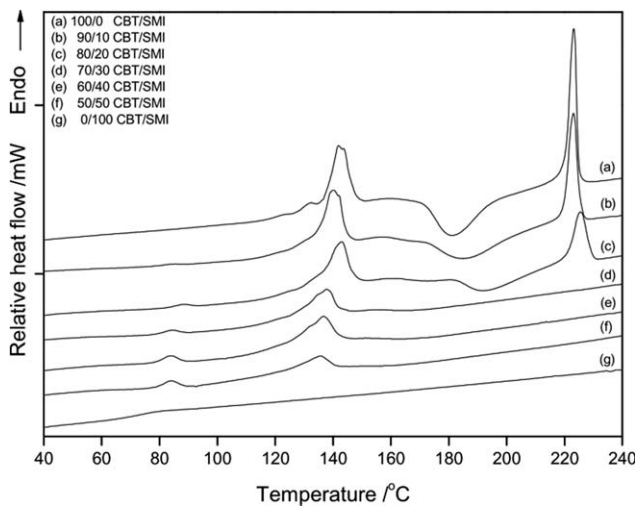

Figure 4 Thermal behavior (heating curve) of various compositions CBT/SMI blends.

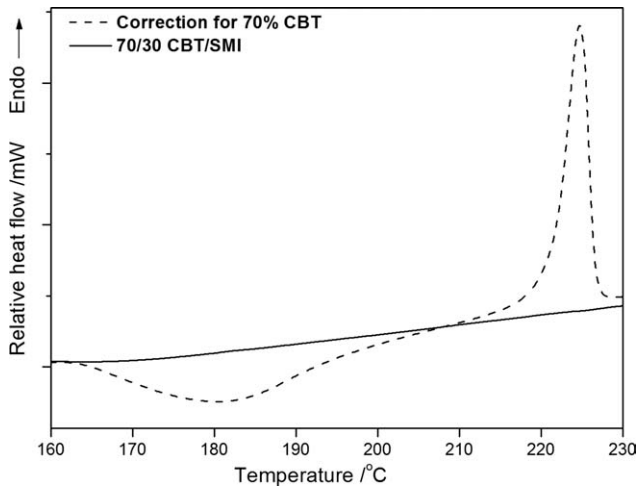

Figure 5 Comparison on first dynamic run between 70/30 CBT/SMI blends and pure CBT oligomers.

Several trends are apparent. Beginning with the T_g of SMI, it is clear that the prominence of the transition increases with increasing SMI content in the blend (as would be expected given the variation in composition). A related trend in the melting region of CBT is also apparent. Again, this variation with blend composition is due to the effect of a gradual decrease in CBT content in the blend.

Examination of the crystallization region of the CBT component shows that the process is clearly being affected by the addition of the SMI component. The effect is most striking in trace (d)—the 70/30 CBT/SMI blend. At this composition, the crystallization process of c-PBT is being hindered by the presence of the SMI component. Although it should be noted that this is only true within the context of the heating rate adopted in this experiment, it cannot be concluded that crystallization is prevented entirely, only that the crystallization process cannot occur over the timescale of the DSC experiment in question. The same is true for compositions above 30 wt % SMI. The decrease in the intensity of the melting peak can be explained in terms of a reduction in the quantity of crystalline material in the sample with increasing SMI content.

Given that the variation in the prominence of the SMI T_g and CBT T_m have been ascribed to the effect of the compositional variation in the blend, it was deemed important to rule-out these effects in the interpretation of the melting of the c-PBT component. Figure 5 shows the thermal response of a 14 mg sample of CBP (dashed line), in which crystallization and melting are clearly prominent. The solid line in Figure 5 represents the thermal response of a 20 mg sample of CBT/SMI blend. This trace is identical to the same region shown in trace (d) in Figure 4, i.e., there is no evidence of crystallization and melting. The reason for selecting a mass of 20 mg was to ensure the masses of the crystallizable components in each sample were identical and that compositional effects could be accounted for. Since the traces were markedly different, it was concluded that the crystallization of c-PBT was indeed hindered by the SMI component.

Additional supporting evidence for the suppression of crystallization in c-PBT by the presence of SMI was obtained by heating the CBT/SMI blend through the CBT melting region to a hold temperature of 190°C. Figure 6 shows the variation of heat flow with time for blends in the composition range (CBT/SMI) 100/0 to 50/50. Over the range of 100/0 to 70/30 there is clear evidence of an exothermic crystallization process, but above 30 wt % SMI, the crystallization process cannot be detected. Again, this suppression of crystallization only applies in the context of this DSC experiment, i.e., at 190°C; the crystallization process is either prevented or becomes too slow for the DSC to detect at compositions above 30 wt % SMI.

The suppression of crystallization by the addition of another polymer may be explained in terms of the formation of what is initially a miscible blend. As a result of the development of some degree of miscibility, the crystallization of c-PBT will require an initial phase-separation stage which will hinder the process through an increase in the induction time for crystallization. This can be seen to some degree in Figure 6 in trace (c). Similar results were obtained by Tripathy et al.,[5] where they found that during *in situ* blending of c-PBT with PVB, the crystallinity c-PBT was suppressed by the blending process, which initially created a miscible blend, which in turn affected the crystallization process. Since no oligomer melting was detected during the second heating of the blends (d)–(e) shown in Figure 6, in was concluded that polymerization had still taken place.

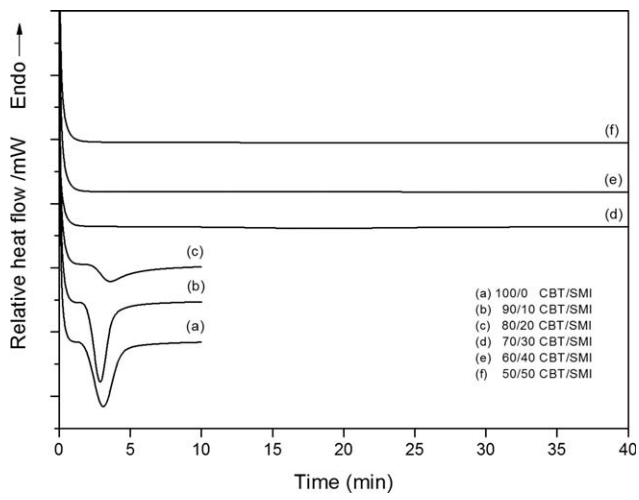

Figure 6 *In situ* polymerization of CBT/SMI Blends at 190°C.

TABLE I
Glass Transition Temperature (T_g) of c-PBT/SMI Blends

Blend composition (c-PBT/SMI) (wt %)	T_g (K)
100/0	300
80/20	303
50/50	316
40/60	325
30/70	328
20/80	333
10/90	336
0/100	348

Glass transition temperature (T_g) of the blends

Miscibility in a polymer blend can be demonstrated by showing that a single composition dependent T_g is observed in the blend. This was found to be the case in the c-PBT/SMI blend, and the T_g values of homopolymers and their blends are shown in Table I.

To explore the variation of T_g with blend composition, the measured SMI T_g data were compared with the following relationships,

Fox[31]:

$$\frac{1}{T_g} = \frac{w_1}{T_{g_1}} + \frac{w_2}{T_{g_2}} \tag{1}$$

Gordon–Taylor[32]:

$$T_g = \frac{w_1 T_{g1} + K w_2 T_{g2}}{w_1 + K w_2} \tag{2}$$

in which w_1 and w_2 are the weight fractions of the component polymers, T_{g_1} and T_{g2} are the glass transition temperatures of the component polymers, ΔC_{p_1} and ΔC_{p_2} represent the change in heat capacity on the transformation from glass to liquid and K is an adjustable fitting parameter in which, $K = \frac{\Delta C_{p2}}{\Delta C_{p1}}$.

It is clear from Figure 7 that the best fit of the data was obtained from the Gordon–Taylor relationship. Deviations from the Fox equation may originate from limitations in the applicability of the relationship to this blend system, i.e., the Fox relationship assumes that the ΔC_p values for both polymers are equal and that mixing occurs with no volume expansion. However, the presence of a single composition-dependent T_g clearly indicates the development of miscibility in the c-PBT/SMI blend system.

The depression of equilibrium melting temperatures, T_m^o

Figure 8 shows the variation of the c-PBT melting point (as defined by the last trace of crystallinity) with crystallization temperature. Clearly, the data were amenable to a Hoffman–Weeks analysis in order to determine the equilibrium melting temperature, T_m^o which is defined

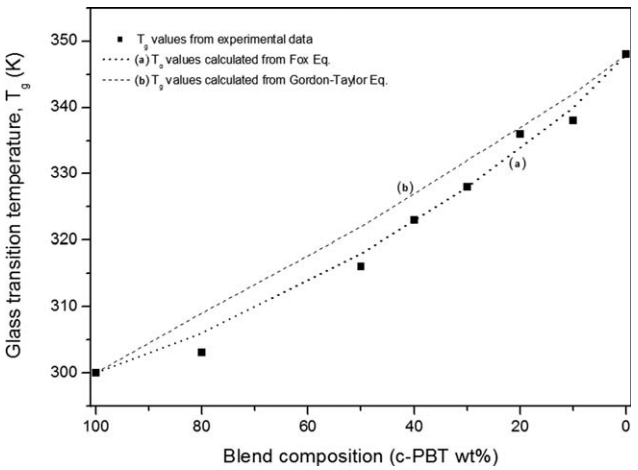

Figure 7 Comparison of experimental T_g data with Fox and Gordon–Taylor relationships in c-PBT/SMI blends.

as the melting temperature of lamellar crystals of an infinite thickness.[33] The variation of T_m with T_c can be described by the following relationship,[34]

$$T_m = T_m^o\left(1 - \frac{1}{2\beta}\right) + \frac{T_c}{2\beta} \tag{3}$$

where $\beta = \sigma_e l / \sigma l_e$ and σ is the fold surface free energy, l is the lamellae thickness and the subscript e refers to equilibrium conditions, and $\beta = 1.0$ in the absence of re-crystallization or annealing during melting. A plot of T_m against T_c should be linear with slope of 0.5. The equilibrium melting temperature can be found from the intersection of the interpolated T_m versus T_c line with the line $T_m = T_c$. Linear regression on the T_m versus T_c lines showed that the slopes were no less than 0.4. This indicates a strong tendency toward melting under equilibrium conditions.

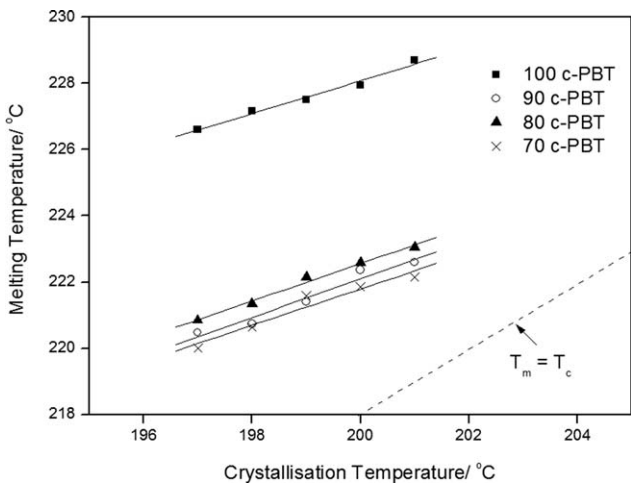

Figure 8 Hoffman–Week's plot of observed melting temperature against crystallization temperature for c-PBT and c-PBT/SMI blends.

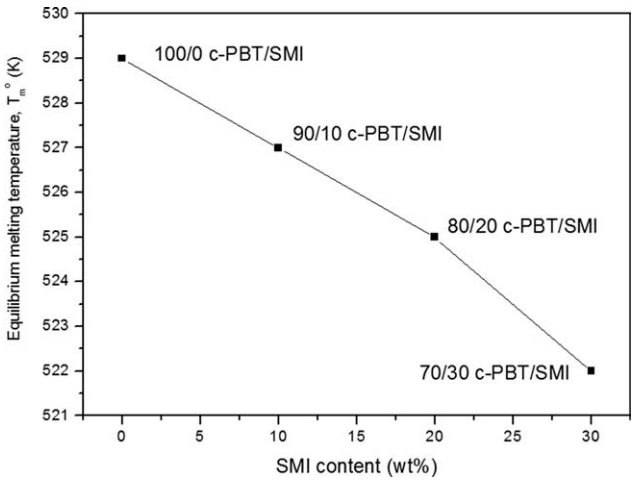

Figure 9 The equilibrium melting temperatures of c-PBT/SMI blends.

Figure 9 shows the variation of the calculated T_m^o with increasing SMI content in the blend. A clear compositional variation was observed with the calculated values for T_m^o decreasing with increasing SMI content. Depression of the T_m^o in polymer blend systems has been reported previously and has been ascribed to the effects of miscibility.[35–37] Consequently, the trend shown in Figure 9 clearly supports the idea that the c-PBT/SMI blend system is miscible when both components are amorphous. To enable the c-PBT/SMI blend miscibility to be quantified, the data presented in Figure 9 were analyzed using the theory proposed by Nishi and Wang[23] and Nishi et al.,[24] which is expressed as follows,

$$\frac{1}{T^o_{m(\text{blend})}} - \frac{1}{T^o_{m(\text{pure})}} = \frac{-RV_2}{\Delta H_f^o V_1}\left[\frac{In\varphi_2}{m_2} + \left(\frac{1}{m_2} - \frac{1}{m_1}\right)\varphi_1 + \chi_{12}\varphi_1^2\right] \quad (4)$$

where, T_m^o is equilibrium melting temperature, ΔH_f^o is the heat fusion for the 100% crystalline component, R is the universal gas constant, V is the molar volume of the polymer repeating unit, m is the degree of polymerization, χ_{12} is the polymer–polymer interaction parameter and φ is the volume fraction of the component in the blend. The subscripts 1 and 2 denote the non-crystallizable and crystallizable components, respectively. The volume fraction, φ can be calculated from the weight fractions and densities of the components using the following expression,

$$\varphi_1 = \frac{w_1/\rho_1}{w_1/\rho_1 + w_2/\rho_2} \quad (5)$$

In order to simply the application of this theory, it is commonly assumed that the degrees of polymerization of both component polymers are approximately equal and that both values tend to infinity.[38,39] In this case eq. (4) can be reduced to the following expression,

$$\frac{1}{T^o_{m(blend)}} - \frac{1}{T^o_{m(\text{pure})}} = \frac{-RV_2}{\Delta H_f^o V_1}\left(\chi_{12}\varphi_1^2\right) \quad (6)$$

If a blend is miscible, a plot of $\frac{1}{T^o_{m(\text{blend})}} - \frac{1}{T^o_{m(\text{pure})}}$ against φ_1^2 should yield a straight line of negative slope, the value of which represents the interaction parameter, χ_{12}. In order to apply eq. (6), the following parameters were used; $\Delta H_f^o = 85.75$ J g^{-1},[8,40] $R = 8.314$ J K^{-1} mol^{-1}, $V_1 = 251.2$ cm^3 mol^{-1} of monomer, $V_2 = 129.6$ cm^3 mol^{-1} of monomer, $\rho_1 = 1.14$ g cm^{-3},[41] and $\rho_2 = 1.32$ g cm^{-3}.[42] Figure 10 shows a Nishi–Wang plot from which a value of -3.67×10^{-2} has been calculated for the interaction parameter. In conjunction with the presence of single, composition-dependent T_g and the depression of the T_m^o, the negative value of the χ_{12} parameter found in this study indicates that the c-PBT and SMI blend system is miscible.

Further supporting evidence for the suppression of crystallinity was observed in the fracture surfaces of the blends. Figure 11 shows the fracture surfaces of two blends that have been subjected to a polymerization time of 30 min. In the case of the 80/20 C-PBT/SMI blend [Fig. 11(A)] there is clear evidence of the formation of rod-like crystallites, but in the case of the 20/80 blend [Fig. 11(B)], no such crystallites were apparent and the blend fracture surface appears homogeneous.

CONCLUSIONS

Blends of CBT oligomers and SMI were prepared using a solid dispersion technique followed by

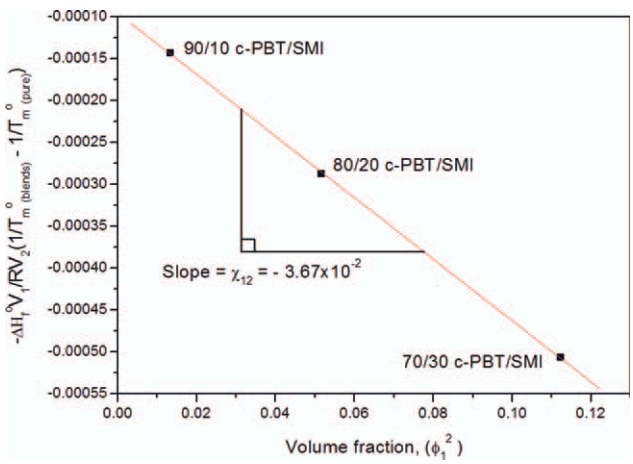

Figure 10 Application of Flory–Huggins theory modified by Nishi–Wang equation to c-PBT/SMI blends. [Color figure can be viewed in the online issue, which is available at wileyonlinelibrary.com.]

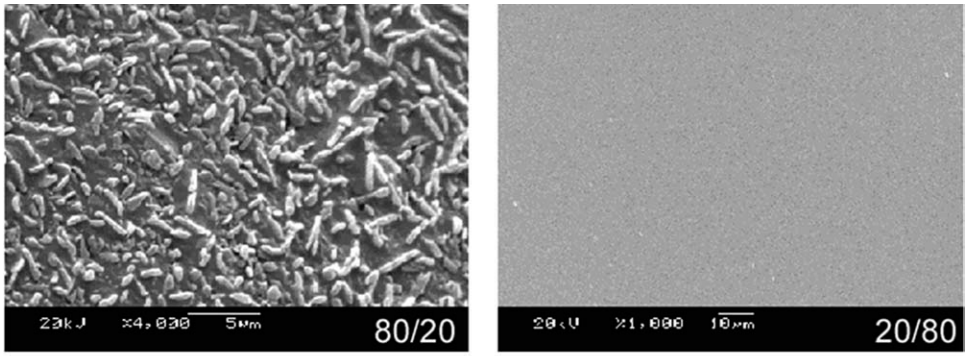

A-(80/20 c-PBT/SMI) B-(20/80 c-PBT/SMI)

Figure 11 The morphology of c-PBT rich and SMI rich blend.

in situ polymerization of the CBT oligomers to produce a blend of c-PBT polymer and SMI. Preparation of the blends within the DSC showed that under the conditions of the DSC experiment, the crystallization of c-PBT was suppressed by the presence of SMI. This was most apparent at compositions in excess of 30 wt % SMI, at which point, the crystallization process of c-PBT became undetectable within the context of the conditions adopted for the DSC experiment. A single, composition-dependent blend T_g was also found which strongly suggested that the blend was miscible. Furthermore, the negative value of the Flory–Huggins interaction parameter (χ_{12}), observed in this study indicates that c-PBT and SMI pairs are thermodynamically miscible in the melt. The presence of miscibility offers an explanation of why the crystallization process in c-PBT became depressed: miscibility necessitated a phase separation process prior to the crystallization. This manifested itself as an induction time for the crystallization to such an extent that the crystallization process became undetectable in the context of the *in situ* polymerization process adopted in this work. Further work will focus on a kinetic analysis of the crystallization process of c-PBT from the blend of c-PBT and SMI.

The authors thank Professor William J. MacKnight for advice and Mr. F. Biddlestone for technical support and assistance.

References

1. Miller S. Macrocyclic polymer from cyclic oligomers of polybutylene terephthalate, Ph. D. Dissertation, University of Massachusetts, 1998.
2. Youk, J. H.; Boulares, A.; Kambour, R. P.; MacKnight, W. J. Macromolecules 2000, 33, 3600.
3. Youk, J. H.; Kambour, R. P.; MacKnight, W. J. Macromolecules 2000, 33, 3594.
4. Youk, J. H.; Kambour, R. P.; MacKnight, W. J. Macromolecules 2000, 33, 3606.
5. Tripathy, A. R.; Chen, W.; Kukureka, S. N.; MacKnight, W. J. Polymer 2003, 44, 1835.
6. Tripathy, A. R.; Burgaz, E.; Kukureka, S. N.; MacKnight, W. J. Macromolecules 2003, 36, 8593.
7. Tripathy, A. R.; MacKnight, W. J.; Kukureka, S. N. Macromolecules 2004, 37, 6793.
8. Tripathy, A. R.; Elmoumni, A.; Winter, H. H.; MacKnight, W. J. Macromolecules 2005, 38, 709.
9. Brunelle, D. J.; Bradt, J. E.; Serth-Guzzo, J.; Takekoshi, T.; Evans, T. L.; Pearce, E. J.; Wilson, P. R. Macromolecules 1998, 31, 4782.
10. Parton, H.; Baetsa, J.; Lipnikc, P.; Goderisb, B.; Devauxc, J.; Verpoest, I. Polymer 2005, 46, 9871.
11. Parton, H.; Verpoest, I. Polym Compos 2005, 26, 60.
12. Mohd Ishak, Z. A.; Shang, P. P.; Karger-Kocsis, J. J Therm Anal Calorim 2006, 84, 637.
13. Nachlis, W. L.; Kambour, R. P.; MacKnight, W. J. Polymer 1994, 35, 3643.
14. Nachlis, W. L.; Bendler, J. T.; Kambour, R. P.; MacKnight, W. J. Macromolecules 1995, 28, 7869.
15. Kotnis, M. A.; Muthukumar, M. Macromolecules 1992, 25, 1716.
16. Baets, J.; Dutoit, M.; Devaux, J.; Verpoest, I. Composites: Part A 2008, 39, 13.
17. Baets, J.; Godara, A.; Devaux, J.; Verpoest, I. Composites: Part A 2008, 39, 1756.
18. Bardash, L.; Boiteux, G.; Seytre, G.; Hakme, C.; Dargere, N.; Rybak, A.; Melis, F. E-Polymers 2008, 1, 155.
19. Tripathy, A. R.; Farris, R. J.; MacKnight, W. J. Polym Eng Sci 2007, 47, 1536.
20. Mohd Ishak, Z. A.; Leong, Y. W.; Steeg, M.; Karger-Kocsis, J. Compos Sci Technol 2007, 67, 390.
21. Berti, C.; Fiorini, M.; Sisti, L. Eur Polym J 2009, 45, 70.
22. Jiang, Z. Y.; Siengchin, S.; Zhou, L. M.; Steeg, M.; Karger-Kocsis, J.; Man, H. C. Composites: Part A 2009, 40, 273.
23. Nishi, T.; Wang, T. T. Macromolecules 1975, 8, 909.
24. Nishi, T.; Wang, T. T.; Kwei, T. K. Macromolecules 1975, 8, 227.
25. Phelps. Species modification in macrocyclic polyester oligomers and compositions prepared thereby, U.S. Patent, 6,436,548, 2002.
26. Gabbott, P., Ed. Principles and Applications of Thermal Analysis; Blackwell Publishing Ltd: Oxford, UK, 2008.
27. Bryant, J. J. L.; Semlyen, J. A. Polymer 1997, 38, 4531.
28. Mohd Ishak, Z. A.; Gatos, K. G.; Karger-Kocsis, J. Polym Eng Sci 2006, 46, 743.
29. Brunelle, D. J. In Modern Polyesters: Chemistry and Technology of Polyester and Copolyesters; Scheirs, J., Long, T. E., Eds.; Wiley: New York, 2003, 117.

30. Brunelle, D. J.; Shannon, T. G. Macromolecules 1991, 24, 3035.
31. Fox, T. G. Bull Am Phys Soc 1956, 1, 123.
32. Gordon, M.; Taylor, J. S. J Appl Chem 1952, 2, 493.
33. Lim, J. S.; Noda, I.; Im, S. S. Eur Polym J 2008, 44, 1428.
34. Hoffman, J. D.; Weeks, J. J. J Res Natl Bur Stand 1961, 66, 13.
35. Xing, P. X.; Dong, L. S.; An, Y. X.; Feng, Z. L.; Avella, M.; Martuscelli, E. Macromolecules 1997, 30, 2726.
36. Chen, H. L.; Porter, R. S. J Polym Res Taiwan 1999, 6, 21.
37. El-Shafee, E.; Saad, G. R.; Fahmy, S. M. Eur Polym J 2001, 37, 2091.
38. Zhang, H. L.; Ren, M. Q.; Chen, Q. Y.; Sun, S. L.; Sun, X. H.; Zhang, H. X.; Mo, Z. S. J Polym Sci Part B: Polym Phys 2006, 44, 1320.
39. Utracki, L. A. Polymer Alloys and Blends: Thermodynamic and Rheology; Hanser Publishers: Munich, Vienna, New York, 1989.
40. Yokouchi, M.; Sakakibara, Y.; Chatani, Y.; Tadokoro, H.; Tanaka, T.; Yoda, K. Macromolecules 1976, 9, 266.
41. Moore, E. R.; Pickelman, D. M. Ind Eng Chem Prod Res Dev 1986, 25, 603.
42. Fakirov, S., Ed. Handbook of Thermoplastic Polyesters, Wiley-VCH: Weinheim, 2002.